Journal of Physiology

C-type inactivation involves a significant decrease in the intracellular aqueous pore volume of Kv1.4 K⁺ channels expressed in *Xenopus* oocytes

XueJun Jiang *†, Glenna C. L. Bett *, XiaoYan Li *†, Vladimir E. Bondarenko * and Randall L. Rasmusson *

* Department of Physiology and Biophysics, School of Medicine and Biomedical Sciences, 124 Sherman Hall, State University of New York at Buffalo, Buffalo, NY 14214-3005, USA and † Department of Cardiology, Renmin Hospital of Wuhan University, 238 Jiefang Road, Wuhan, Hubei, China 430060

Channels are water-filled membrane-spanning proteins, which undergo conformational changes as they gate, i.e. open or close. These conformational changes affect both the shape of the channel and the volume of the water-filled pore. We measured the changes in pore volume associated with activation, deactivation, C-type inactivation and recovery in an N-terminal-deleted mutant of the Kv1.4 K⁺ channel (Kv1.4ΔN) expressed in *Xenopus* oocytes. We used giant-patch and cut-open oocyte voltage clamp techniques and applied solutes which are too large to enter the pore mouth to exert osmotic pressure and thus favour smaller pore volume conformations. Applied intracellular osmotic pressure (300 mM sucrose) sped inactivation (time constants ($\tau_{inactivation}$): control, 0.66 ± 0.09 s; hyperosmotic solution, 0.29 ± 0.04 s; $n = 5$, $P < 0.01$), sped deactivation ($\tau_{deactivation}$: control, 18.8 ± 0.94 ms; hyperosmotic solution, 8.01 ± 1.92 ms; $n = 5$, $P < 0.01$), and slowed activation ($\tau_{activation}$: control, 1.04 ± 0.05 ms; hyperosmotic solution, 1.96 ± 0.31 ms; $n = 5$, $P < 0.01$). These effects were reversible and solute independent. We estimated the pore volume change on inactivation to be about 4500 Å³. Osmotic pressure had no effect when applied extracellularly. These data suggest that the intracellular side of the pore closes during C-type inactivation and the volume change is similar to that associated with activation or deactivation. This is also similar to the pore volume estimated from the crystal structure of KcsA and MthK K⁺ channels. Intracellular osmotic pressure also strongly inhibited re-opening currents associated with recovery from inactivation, which is consistent with a physical similarity between the C-type inactivated and resting closed state.

C-type inactivation is the result of a major conformational change in K⁺ channels that can determine the ionic dependence, drug affinity and use-dependent drug binding properties of the channels (Lopez-Barneo *et al.* 1993; Baukrowitz & Yellen 1996*a*,*b*; Wang *et al.* 1997, 2003; Rasmusson *et al.* 1998; Ficker *et al.* 1998). C-type inactivation is the rate limiting step for recovery from inactivation of K⁺ channels and is thought to be closely related to the mechanism responsible for 'slow' inactivation of calcium and sodium channels (Zhang *et al.* 1994; Qu *et al.* 1999; Todt *et al.* 1999). C-type inactivation is sensitive to the concentration of extracellular permeant ions (Lopez-Barneo *et al.* 1993; Rasmusson *et al.* 1998), competes with extracellular TEA (Armstrong, 1971; Hoshi *et al.* 1990; Lipkind *et al.* 1995) and is sensitive to mutations near the extracellular mouth of the channel (Hoshi *et al.* 1991; Busch *et al.* 1991; Balser *et al.* 1996; Liu *et al.* 1996; Ficker *et al.* 1998). Based on this evidence, C-type inactivation was thought to arise from a closure of the extracellular mouth of the pore (Baukrowitz & Yellen, 1995, 1996*b*; Ficker *et al.* 1998). However, C-type

inactivation is strongly influenced by events occurring at the intracellular side of the pore (Rasmusson *et al.* 1995; Wang *et al.* 2003; Li *et al.* 2003).

Channels are membrane-spanning water-filled pores. As the channel transitions between non-conducting and conducting states the structure, and therefore the volume, of the water-filled pore changes. If non-conducting osmolytes are introduced on one side of the membrane, there will be an increase in osmotic pressure. Frog oocyte membranes are relatively impermeable to water compared to other eukaryotic cells, which allows the osmotic pressure to be manipulated independently on either side of the membrane without major transmembrane flow artifacts and associated local unstirred layer effects (Starkus *et al.* 1995; Zeuthen *et al.* 2002). If osmolytes are chosen so that they are too large to enter the channel vestibule there will be an imbalance and an osmotic pressure gradient between the water-filled pore and the bath solution. If the volume of the water-filled pore is greater in the conducting state than the non-conducting

state, an increase in osmotic pressure would favour the closed *versus* the open state (Zimmerberg & Parsegian, 1986). This is illustrated in Fig. 1.

The process of activation is hypothesized to involve the formation of a water-filled intracellular vestibule (Jiang *et al.* 2002). The activation rate should, therefore, be slowed by application of large intracellular solutes. Similarly, an increase in osmotic pressure will favour the closed state and therefore enhance the rate of deactivation (Zimmerberg *et al.* 1990). If C-type inactivation involves a decrease in the volume of the intracellular pore, then an increase in intracellular osmotic pressure will promote the development of C-type inactivation. If the volume changes involved in activation and C-type inactivation are similar then the rates of activation, deactivation and C-type inactivation will be changed proportionately. The percentage change will depend only on the volume changes involved rather than the scale of the parameter values, which are orders of magnitude different.

In this study we demonstrate that the major physical conformational change in terms of pore volume associated with C-type inactivation occurs at the intracellular side of the channel.

METHODS

Mature female *Xenopus laevis* (Xenopus Express, FL, USA) were cared for in accordance with standards approved by the Institutional Animal Care and Use Committee of the University at Buffalo SUNY. Frogs were anaesthetized by immersion in tricaine

solution (1 g l^{-1} Sigma). Oocytes were digested by placing in a collagenase-containing Ca^{2+}-free OR2 solution (mM: 82.5 NaCl, 2 KCl, 1 MgCl$_2$, 5 Hepes (pH 7.4); 1 mg ml^{-1} collagenase (type I, Sigma) added). The oocytes were gently shaken for 1.5–2 h, with an enzyme solution replacement at 1 h. Defolliculated oocytes (stage V–VI) were injected (using the Nanoject microinjection system; Drummond Scientific Co., Broomall, PA, USA) with up to 50 ng mRNA of a Kv1.4 channel clone (Kv1.4ΔN) originally isolated from ferret heart (Comer *et al.* 1994). Frogs were humanely killed by overdose of anaesthetic through immersion following the final collection of oocytes.

Currents were recorded at room temperature (~22 °C). Two procedures were used: the cut-open oocyte voltage clamp and the giant-patch technique. Cut-open oocyte experiments (Bezanilla *et al.* 1991) were performed using a CA-1B Amplifier (Dagan Corp., Minneapolis, MN, USA). Oocytes were permeabilized with a 1 % saponin solution. Microelectrodes with resistances of 0.5–1.5 MΩ (when filled with 3 M KCl) were fabricated from 1.5 mm o.d. borosilicate glass tubing (TW150-4, WPI) using a two-stage puller. The control extracellular solution (98 K) contained (mM): 0 NaCl, 98 KCl, 1 MgCl$_2$, 1.8 CaCl$_2$, and 10 Hepes (pH adjusted to 7.4 with KOH). The intracellular solution contained (mM): 98 KCl, 1 MgCl$_2$, 1.8 EGTA, and 10 Hepes (pH adjusted to 7.4 with KOH). Control cut-open oocyte currents averaged 3.75 ± 2.60 nA (mean ± S.D., $n = 7$).

Giant torn-off patches (Hilgemann, 1990) were taken from some oocytes and used as inside-out membrane patches in which intracellular solutions were controlled by a rapid solution-switching device (ALA Scientific Instruments Inc., NY, USA). Microelectrodes (0.5 MΩ) were coated with a mixture containing 5 % parafilm and light mineral oil. The giant-patch electrode solution contained (mM): 98 KCl, 1 MgCl$_2$, 2.5 CaCl$_2$, 10 Hepes (pH adjusted to 7.4 with KOH). For giant-patch experiments, the
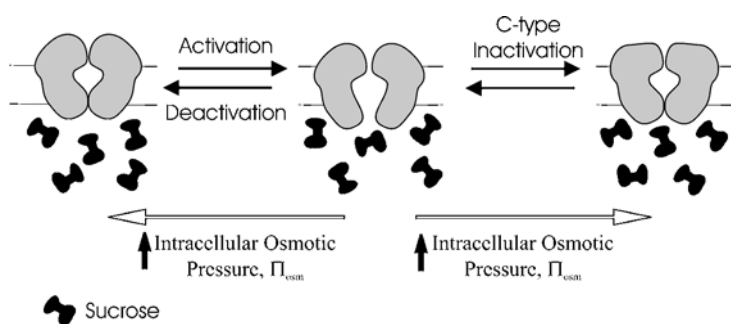
Figure 1. The effect of osmostic pressure on ion channel behaviour

When a solute too large to enter the pore mouth is added to the solution on one side of the membrane osmosis will result in withdrawal of water from the pore. There will be a resulting osmotic pressure on the channel, which will make channel states with smaller pore volumes more energetically favourable. Activation of voltage-dependent cation channels is believed to result in the formation of a large intracellular vestibule but involve only relatively minor changes in volume on the extracellular face (Jiang *et al.* 2002). Activation, therefore, should be relatively insensitive to applied extracellular osmotic pressure. C-type inactivation is thought to involve closure of the extracellular side of the pore. If this closure involves a substantial change in volume, then extracellular osmotic pressure should promote C-type inactivation. Activation involves the formation of a large water-filled intracellular vestibule. Therefore it should be relatively sensitive to applied intracellular osmotic pressure, with higher osmotic pressure favouring the closed state. Deactivation is the reverse process to activation, so should be affected by osmotic pressure to a similar degree. If C-type inactivation involves a substantial change in intracellular pore volume, then intracellular osmotic pressure should promote C-type inactivation. If the volume changes involved in activation/deactivation and C-type inactivation are similar then the rates of activation, deactivation, and C-type inactivation should be changed proportionately, despite their vastly different time scales.

initial bath solution contained (mM): 98 KCl, 1.8 MgCl$_2$, 1 EGTA, 10 Hepes (pH adjusted to 7.4 with KOH). Sucrose (300 mM) or *N*-methyl-D-glucamine methanesulfonate (NMDG, 300 mM) was added to the solutions to vary the osmotic pressure. Changes in kinetic properties with osmotic pressure were all measured relative to behaviour in the same patch under control conditions. Giant-patch peak currents at +30 mV were 3.19 ± 0.53 nA (mean ± S.D.) in control and 1.37 ± 0.36 nA (mean ± S.D.) in 300 mM NMDG ($n = 5$).

Data were digitized and analysed using pCLAMP 7 (Axon Instruments, CA, USA). Further analysis was performed using Clampfit (Axon Instruments, CA, USA), Excel (Microsoft Corp., WA, USA) and Origin (Microcal Software Inc., MA, USA). Data were filtered at 2 kHz and reported as means ± S.E.M. unless stated otherwise). Confidence levels were calculated using Student's paired *t* test. The null hypothesis was rejected when $P < 0.05$. Currents were inverted for clarity where necessary (see individual figure legends).

Structural modelling was performed using the Insight II 3D graphical environment for molecular modelling (Accelrys Inc., San Diego, CA, USA) running on a Silicon Graphics Indigo workstation (SGI, CA, USA) with a UNIX operating system. Atom co-ordinates were downloaded from the Research Collaboratory

for Structural Bioinformatics. Side-chains were replaced using sequence homology modelling (Vector NTI, Informax, Inc., MD, USA) and energy minimized in Insight II. Cross-sectional areas of the pore were estimated in 1 Å (0.1 nm) steps along the axis of the pore of each channel type after side-chain substitution for Kv1.4 and energy minimization of side-chain orientation. Pore dimensions were estimated from the Van der Waal radius of the innermost side-chain carbon atom corrected for an attached hydrogen. These were summed to estimate the aqueous volume of the pore.

RESULTS

Electrophysiology

Kv1.4ΔN channels (amino acids 2–146 are deleted from the N-terminal which removes N-type inactivation) inactivate only by C-type inactivation, so providing an excellent system to study the effects of osmotic pressure on C-type inactivation. We studied these channels expressed in *Xenopus* oocytes. Osmotic pressure was manipulated by adding sucrose or NMDG to the intracellular or extracellular solutions, and the kinetic behaviour of Kv1.4ΔN was studied.
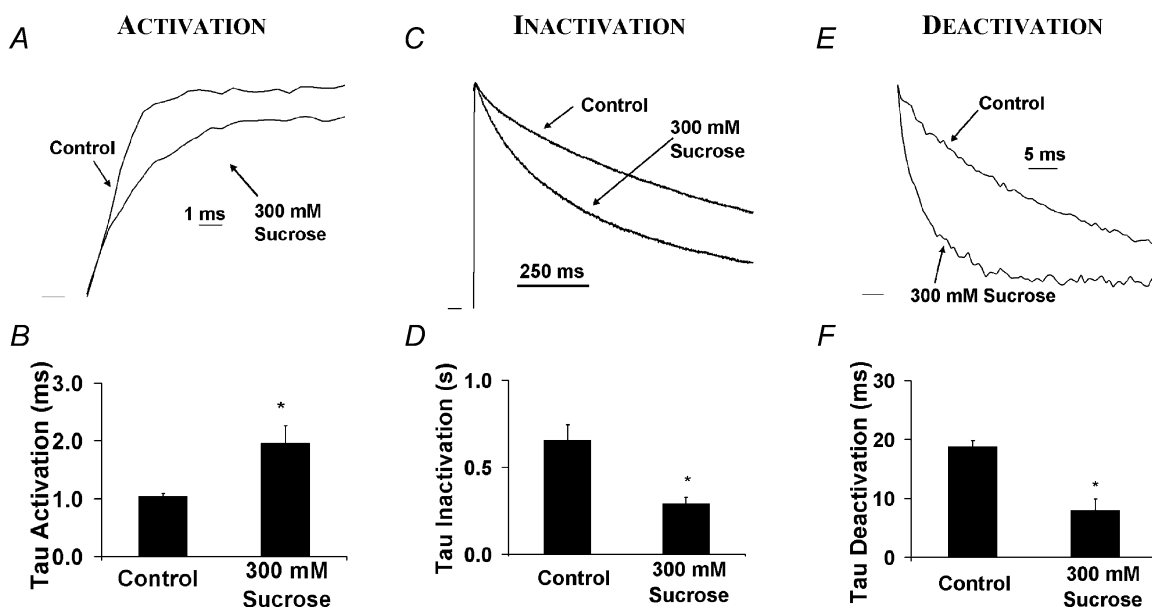

Figure 2. Effect of intracellular hyperosmotic pressure on activation, C-type inactivation and deactivation in Kv1.4ΔN channels

Currents were recorded from detached inside-out giant patches (Hilgemann, 1990) perfused with 300 mM (330 mosmol l^{-1}) sucrose to increase osmotic pressure. Currents are normalized (and inverted where necessary) to emphasize changes in kinetic rates.. Voltage clamp pulses (duration 1 s were applied from −90 to +50 mV. *A*, activation was slowed in the presence of an intracellular hyperosmotic solution. *B*, the activation time constant (τ) increased from 1.04 ± 0.05 ms in control to 1.96 ± 0.31 ms in hyperosmotic solution ($n = 5$, $P < 0.01$). *C*, the rate of C-type inactivation increased in intracellular hyperosmotic solution. *D*, the C-type inactivation time constant decreased from 0.66 ± 0.09 s in control to 0.29 ± 0.04 s in hyperosmotic solution ($n = 5$, $P < 0.01$). *E*, deactivation increased with intracellular hyperosmotic exposure. *F*, the fast time constant of deactivation decreased from 18.8 ± 0.94 ms in control to 8.01 ± 1.92 ms in hyperosmotic solution ($n = 5$, $P < 0.01$). Peak current was also suppressed by application of hyperosmotic pressure (see volume calculations). Peak current was 3.22 μA in control and 1.69 μA in 300 mM sucrose. Peak currents elicited in hyperosmotic solutions were 51 ± 6 % (at +50 mV) 46 ± 5 % (+40 mV) and 43 ± 6 % (+30 mV) of control ($n = 5$).

Figure 2 shows the effect of exposing Kv1.4ΔN channels to a hyperosmotic intracellular solution made with 300 mM sucrose. The time constant (τ) of activation was estimated by a single exponential fit to the late phase of current activation, which followed the initial sigmoid delay. Using the giant-patch voltage clamp technique to perfuse oocytes with a hyperosmotic intracellular solution resulted in a slowing of activation (Fig. 2*A* and *B*): the time constant of activation ($\tau_{activation}$) was increased from 1.04 ± 0.05 ms in control to 1.96 ± 0.31 ms in hyperosmotic solution ($n = 5$, $P < 0.01$). This is consistent with previous observations on a related delayed rectifier K^+ channel (Zimmerberg *et al.* 1990) and a more distantly related Na^+ channel (Rayner *et al.* 1992). This observation is also consistent with the hypothesis that activation involves the creation or opening of an intracellular water-filled vestibule.

The rate of deactivation was increased by an intracellular hyperosmotic solution, with the fast time constant of deactivation ($\tau_{deactivation}$) reduced from 18.8 ± 0.94 ms in control to 8.01 ± 1.92 ms in hyperosmotic solution ($n = 5$, $P < 0.01$). This result is consistent with the opening and closing of an intracellular water-filled vestibule.

Surprisingly, the rate of C-type inactivation was also increased when the channel was exposed to an intracellular hyperosmotic solution. The time constant of inactivation ($\tau_{inactivation}$) decreased from 0.66 ± 0.09 s in control to 0.29 ± 0.04 s in hyperosmotic solution ($n = 5$, $P < 0.01$). Even though these conformational changes occur on vastly different time scales, the relative changes in all time constants were of a similar size (see Fig. 2). This similarity of kinetic changes with osmotic pressure suggests that the intracellular pore volume change associated with all of these processes was similar. This is not surprising for
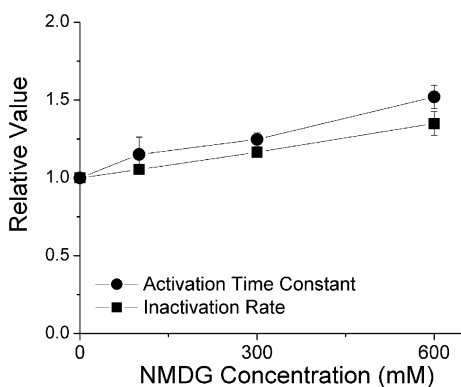
Figure 3. The effects of osmotic pressure were related to the osmolyte concentration

The cut-open oocyte voltage clamp technique was used to apply concentrations of NMDG between 0 and 600 mM, and determine the time constants of activation and inactivation. The oocyte was stepped from -90 to $+30$ mV for 5 s in 0, 100, 300 and 600 mM NMDG ($n = 3$). Activation and C-type inactivation rates are normalized to enable direct comparison.

activation and deactivation, since they are presumably the forward and reverse processes for the same conformational change. However, it is surprising for C-type inactivation. These results suggest that C-type inactivation involves a closure of the intracellular pore of the same physical size as deactivation.

In order to confirm that the effects of sucrose were due to changes in osmotic pressure and not to some specific interaction between sucrose and the channel, the giant-patch experiments shown in Fig. 2 were repeated with 300 mM NMDG as the osmolyte. The changes in gating kinetics were independent of the osmolyte used, with NMDG decreasing the rate of activation, and increasing the rate of deactivation and inactivation. The activation time constant increased from 0.73 ± 0.03 ms in control to 1.18 ± 0.09 ms in hyperosmotic conditions ($n = 5$, $P < 0.01$). The C-type inactivation time constant decreased from 0.72 ± 0.03 s in control to 0.38 ± 0.02 s in hyperosmotic conditions ($n = 5$, $P < 0.01$), and the fast time constant of deactivation decreased from 19.86 ± 1.57 in control to 12.34 ± 1.13 ms in hyperosmotic solution ($n = 5, P < 0.01$).

To ensure that the effects of the osmolytes were due to a change in pressure, and were not a result of the osmolyte binding to the channel, we tested the response of the channel to several osmolyte concentrations in the cut-open voltage clamp configuration. Figure 3 shows that over the range 0–600 mM NMDG there is a linear relationship between the rate of inactivation ($1/\tau$) and the intracellular osmolyte concentration.

Toxin binding near the external mouth of the pore is relatively unaffected by the activation or inactivation state of voltage-gated channels (Naranjo & Miller, 1996). Although the processes of activation and C-type inactivation undoubtedly result in changes in the structure of the outer mouth of the pore, the toxin binding data suggest that these changes are unlikely to be as physically large as the conformational changes associated with the intracellular gate. We confirmed this prediction through addition of 300 mM sucrose to the extracellular solution in the cut-open clamp configuration. External osmotic pressure had no effect on activation, only a small (but statistically significant) effect on deactivation, and no significant effect on C-type inactivation (Fig. 4). Similar results were observed for application of extracellular NMDG (results not shown). Starkus *et al.* (1995) observed a similar effect of intracellular, but not extracellular, sucrose addition on activation and deactivation rates in *Shaker* B channels. This is consistent with there being little or only very small physical changes in the water-filled volume of the external side of the pore (Perozo *et al.* 1999). In a related K^+ channel, KcsA, an 'external activation gate' is reported to result in a minor change in solvent accessibility (Perozo *et al.* 1999), which is consistent with

the extracellular changes that accompany C-type inactivation. However, a small change in solvent accessibility does not preclude significant changes in the orientation or conformation of residues on the extracellular face during C-type inactivation. We can only conclude that these changes do not result in a large alteration in the external aqueous permeation pathway, which is inaccessible to the added osmolytes. In other words, the lack of an effect of extracellular osmotic pressure suggests that changes in conformation are either very small, or do not result in a change in volume which excludes the applied osmolytes.

The similarity in the changes that osmotic pressure induces in activation, deactivation, and inactivation suggests that these processes are accompanied by similar changes in physical conformation. The Kv1.4ΔN channel has at least four closed states (C), one open (O) and one inactivated state (I), as shown in eqn (A1) in the Appendix (Comer *et al.* 1994):

$$C \rightleftharpoons C \rightleftharpoons C \rightleftharpoons C \rightleftharpoons O \rightleftharpoons I.$$

Many channels can transition directly from non-conducting partially activated states to inactivated states, without passing through the open or conducting state. Similarly, recovery from inactivation can occur through two pathways: either as a direct transition from the inactivated state to a closed (non-conducting deactivated) state, as indicated by arrows in Fig. 5*A*, or through the open state (Demo & Yellen, 1991; Ruppersberg *et al.* 1991). Channels that follow this latter transition will re-open during recovery and produce a measurable re-opening current. The ratio of channels deactivating through these two pathways depends on channel type, inactivation mechanism, ionic conditions and the holding potential (Demo & Yellen, 1991; Ruppersberg *et al.* 1991). Since recovery occurs at approximately the same rate through both pathways (Demo & Yellen, 1991), the main manifestation of the electrically active pathway is a very slowly decaying 'tail current' (I_{tail}) on repolarization, as shown in Fig. 5. If the C-type inactivated state involves closure of the intracellular mouth of the channel, then transitions through the open state, in which the channel mouth must open again will be less favourable when there is applied osmotic pressure. Intracellular osmotic pressure should therefore oppose re-opening and promote the electrically silent transition.
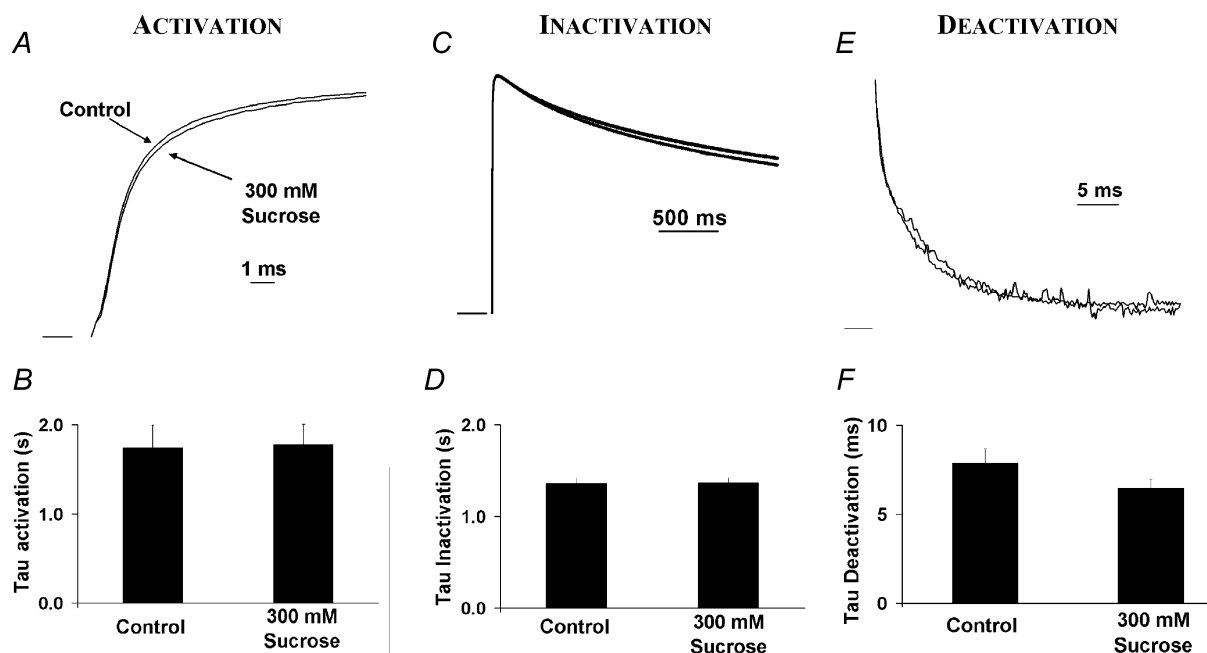
Figure 4. Effect of extracellular osmotic pressure on activation, C-type inactivation and deactivation measured using the cut-open oocyte voltage clamp technique

The hyperosmotic extracellular solution contained 300 mM sucrose, giving an increase in osmotic pressure of 330 mosmol l^{-1}. The membrane was stepped from -90 to $+50$ mV for 1 s. Similar negative results were observed when NMDG was used as the extracellular osmolyte (results not shown). *A*, external hyperosmotic pressure had no effect on activation. *B*, the average time constant of activation was unchanged: $\tau_{activation} = 1.74 \pm 0.26$ ms in control; $\tau_{activation} = 1.78 \pm 0.23$ ms in hyperosmotic solution ($n = 12$, $P > 0.05$). *C*, extracellular hyperosmotic exposure had no effect on C-type inactivation. *D*, the average time constant of inactivation was unchanged: $\tau_{inactivation} = 1.36 \pm 0.06$ s in control; $\tau_{inactivation} = 1.37 \pm 0.06$ s in hyperosmotic solution ($n = 12$, $P > 0.05$) *E*, external hyperosmotic solution had a very small effect on deactivation. *F*, the time constant of deactivation decreased: $\tau_{deactivation} = 7.86 \pm 0.83$ ms in control; $\tau_{deactivation} = 6.46 \pm 0.50$ ms in hyperosmotic solution ($n = 11$, $P < 0.01$).

As predicted, re-opening currents are inhibited by applied intracellular pressure (see Fig. 5). In control conditions, I_{tail} was $0.91 \pm 0.11\%$ of the peak current (I_{peak}), whereas when osmotic pressure was applied I_{tail} was reduced to only $0.03 \pm 0.06\%$ of I_{peak} ($n = 8$, $P < 0.01$). Even though the slow re-opening tail was inhibited by applied intracellular osmotic pressure, the rate of channel recovery was relatively unchanged. This adds further support to the idea that the closed and C-type inactivated states can communicate directly, without requiring re-opening of the intracellular vestibule during deactivation.

Figure 5*D* shows that the recovery from inactivation is essentially unchanged by osmotic pressure. Recovery is controlled by C-type inactivation, so these data indicate that osmotic pressure has promoted normal C-type inactivation. The fact that the ratio of channels going through the closed pathway has been altered by osmotic pressure but the overall recovery from inactivation has not

been changed is consistent with the observations in *Shaker* channels (Demo & Yellen, 1991) that recovery through both the electrogenic and electrically silent pathways occurs at the same rate (Ruppersberg *et al.* 1991).

Structural modelling

We examined the physical implications of our measurements using the Insight II Structural modelling software. We used data from the crystal structure of the open MthK channel (Jiang *et al.* 2002) and the open channel model of KcsA (Doyle *et al.* 1998; Perozo *et al.* 1999) to estimate the available water-filled intracellular volume of the open state (Fig. 6).

We estimate the water-filled volume of the open KcsA pore to be 7431 Å^3 and the open MthK pore to be 7852 Å^3. The values we estimate from our electrophysiological results for the Kv1.4ΔN channel, using a variety of methods (see below) suggest a change of water-filled volume of approximately 55% of this total, consistent with the
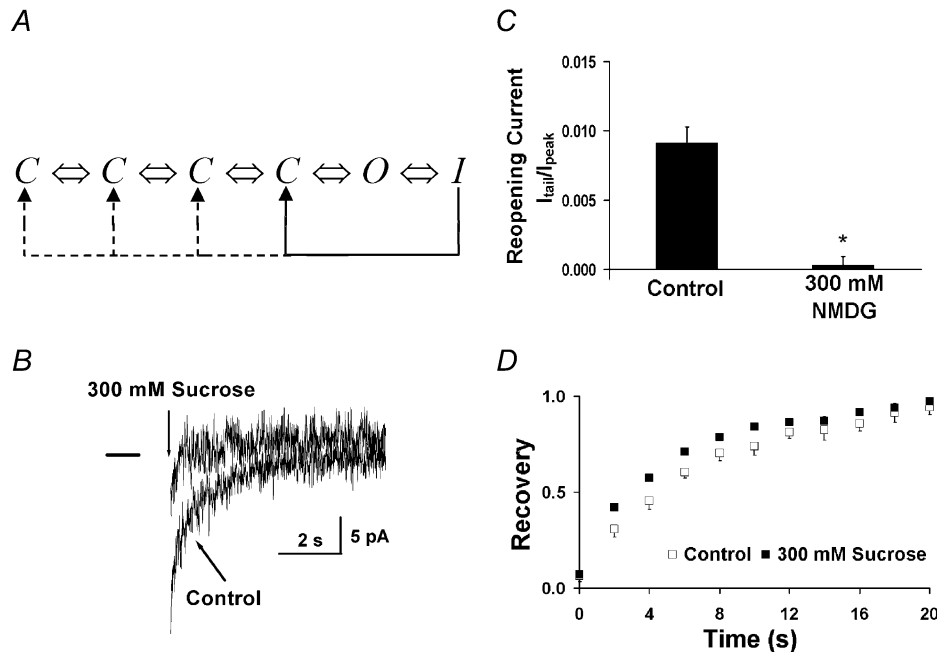
Figure 5. Effect of intracellular osmotic pressure on recovery from inactivation

A, model of the Kv1.4ΔN channel, with four closed states, one open state, and an inactivated state. The channel can recover from the inactivated state by transitioning directly from the inactivated state to the closed state, or by passing through the open state. If the channel recovers by going through the open state, there will be a re-opening current. *B*, effect of applied intracellular pressure on re-opening currents measured using the giant-patch technique. A 5 s depolarizing pulse from −90 to +50 mV was applied to inactivate channels. In control conditions, there was a sustained inward re-opening current (which was a tiny fraction of the fully activated current) as channels slowly recovered from the inactivated state, passed through the open state and subsequently deactivated and returned to the closed state. The re-opening current was inhibited by intracellular osmotic pressure. Deactivation currents are not visible due to the time scale of the sampling rate. Traces were filtered at 40 Hz. *C*, average re-opening currents were inhibited by applied intracellular osmotic pressure. The magnitude of the re-opening current was normalized to the peak current measured during the preceding 500 ms activation pulse to +50 mV. *D*, effect of intracellular osmotic pressure (300 mM sucrose) on recovery from C-type inactivation in giant patches. Applied intracellular osmotic pressure had minimal effect on recovery from inactivation. A 5 s depolarizing pulse (P1) from −90 to +50 mV inactivated the channel. A second pulse to +50 mV (P2) was applied after a variable interval, Δt. Recovery (the ratio of the P2 peak current to the peak P1 current) was plotted against the inter-pulse interval, Δt ($n = 5$).

notion of a small stable internal chamber in the closed KscA channel (Doyle *et al.* 1998). Volume estimates from the structural and mathematical approaches are summarized in Fig. 7.

Mathematical modelling

We used three different approaches to estimate the volume change associated with conformational changes of the Kv1.4ΔN channel. The mathematical derivations are detailed in the Appendix, and only the final equations and estimates of volume changes are presented here.

1. Volume changes associated with C-type inactivation

An estimate of the change in solute-inaccessible aqueous volume can be calculated from the peak current, I_{peak}, and the calculated final current, I_{final} (which is extrapolated from the exponential fit of the experimental current inactivation to infinite time), in the presence and absence of osmotic pressure (π):

$$\Delta V = \frac{kT}{\pi_{osm}} \ln\left(\frac{(I_{final,\pi}/(I_{peak,\pi} - I_{final,\pi})}{(I_{final}/(I_{peak} - I_{final})}\right) \quad (A11)$$

(see Appendix).

Using the values I_{peak} and I_{final} at +30 mV, we estimate that the volume change associated with C-type inactivation is 4652 ± 1469 Å^3 ($n = 5$). The volume change was independent of membrane voltage (see Fig. 7).

2. Volume changes associated with channel activation

For values of peak current near the threshold for activation, i.e. when $P_{open,\pi} < P_{open} \ll 1$, the change in pore volume accompanying activation is related to the peak current by the following equation:

$$\Delta V = -\frac{kT}{\pi_{osm}} \ln\left(\frac{I_{peak,\pi}}{I_{peak}}\right) \quad (A21)$$

(see Appendix).
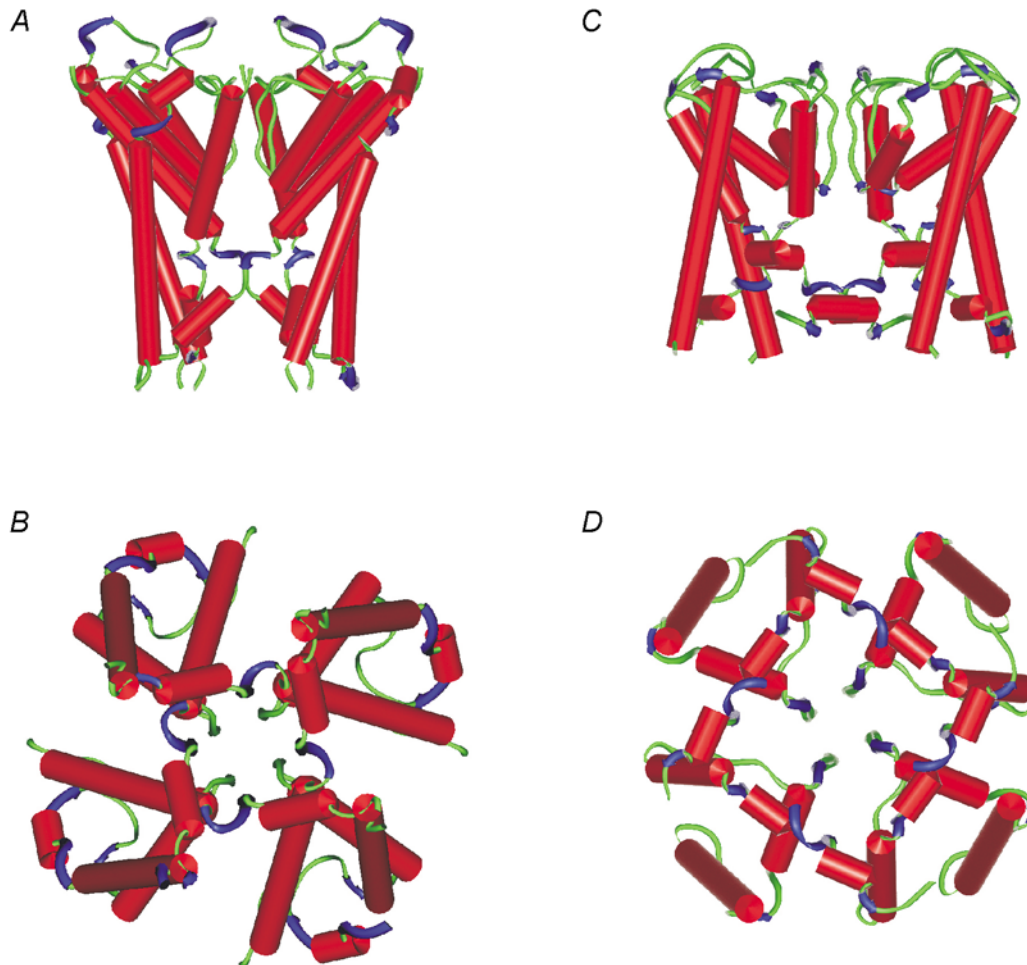
Figure 6. We used manual measurement of the KcsA and MthK intracellular pore dimensions and geometry to estimate the maximum water-filled volume of the entire permeation pathway

A and *B*, side and bottom views of the open KcsA channel (Doyle *et al.* 1998; Perozo *et al.* 1999). *C* and *D*, side and bottom views of the open MthK channel (Jiang *et al.* 2002).

At −30 mV we estimate of the change in pore volume associated with activation to be 3878 ± 1574 Å^3 ($n = 5$). This is similar to the volume calculated for C-type inactivation (see Fig. 7).

3. Kinetic estimates of volume changes

The relationship between rate constants (activation, inactivation and deactivation) and volume change is as follows:

$$\Delta V = \frac{kT}{\pi_{osm}} \ln\left(\frac{\tau}{\tau_\pi}\right) \qquad (A30)$$

(see Appendix).

Using this relationship, we estimate that the volume change associated with inactivation is 4304 ± 980 Å^3 ($n = 5$, measured at +30 mV), activation is 3141 ± 1099 Å^3 ($n = 5$, measured at +30 mV) and deactivation is 5126 ± 1015 Å^3 ($n = 5$, measured at −90 mV).

DISCUSSION

We studied a cloned K$^+$ channel, Kv1.4ΔN, expressed in *Xenopus* oocytes (Comer *et al.* 1994). The gating kinetics of Kv1.4ΔN were sensitive to applied intracellular osmotic pressure: activation was slowed, whereas deactivation and C-type inactivation were speeded. This indicates that C-type inactivation is associated with a decrease in intracellular channel volume. Even though activation, deactivation and C-type inactivation occur on vastly different time scales, the effect of applied osmotic pressure resulted in a similar percentage change in time constants between all three kinetic variables. This suggests that the

Figure 7

Data from five separate mathematical approaches were used to estimate the magnitude of the pore volume change associated with activation (■, rate kinetics; □, current ratio), inactivation kinetics (●, rate kinetics; ○, steady state inactivation) and deactivation kinetics (▲). The estimates were voltage independent. Data from the crystal structure of the open MthK channel (Jiang *et al.* 2002) and the open channel model of KcsA (Doyle *et al.* 1998; Perozo *et al.* 1999) were used to give an estimate the available water-filled intracellular volume of the open state: the open KcsA pore was calculated to be 7431 Å^3 (✕) and the open MthK pore was calculated to be 7852 Å^3 (✳).
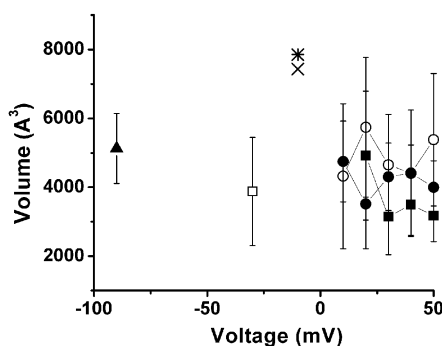
volume change associated with channel opening and closing is similar to that involved in C-type inactivation.

In contrast to the results seen with intracellular changes in osmotic pressure, manipulating extracellular osmotic activity had virtually no effect on activation and a small but statistically significant decrease in the time constant of deactivation. This is similar to observations from other voltage-gated channels, where little or no volume change occurred during activation on the extracellular face as measured both by osmotic pressure (Zimmerberg *et al.* 1990; Rayner *et al.* 1992) and toxin binding (Naranjo & Miller, 1996). Similarly, no change in the rate of C-type inactivation was measured, suggesting that little or no volume changes occur during C-type inactivation on this side of the membrane.

The similarity in changes in water-accessible volume between activation, deactivation and C-type inactivation strongly suggests that the intracellular pore volume change during C-type inactivation is similar to that undergone when the channel changes between the closed and open states.

What other data exist to support this view of C-type inactivation? Basically, the data parallel those used to implicate external pore mouth changes in C-type inactivation. For example, removal of [K$^+$]$_o$ has been shown to speed C-type inactivation, an observation that led to the 'foot in the door' hypothesis of C-type inactivation (Armstrong, 1971). Reduction of [K$^+$]$_i$ has been reported to increase the rate of C-type inactivation in N-terminal deleted *Shaker* potassium channels (Baukrowitz & Yellen, 1996*b*). These results were interpreted as being due to intracellular K$^+$ diffusing through the pore to reach an unstirred layer near the extracellular domain of these channels. We performed similar substitution experiments in Kv1.4ΔN channels in the presence of 98 mM [K$^+$]$_o$ (Li *et al.* 2003); the earlier experiments by Baukrowitz & Yellen (1996*b*) were performed with 0 mM [K$^+$]$_o$. With 98 mM [K$^+$]$_o$, the extracellular site for potassium modulation of C-type inactivation should be saturated and any effects of potassium removal should reflect changes in intracellular interactions. Substitution of intracellular 98 mM [K$^+$]$_i$ with 98 mM [NMDG]$_i$ resulted in a significant increase in the rate of C-type inactivation ($\tau_{inactivation}$: control, 0.84 ± 0.11 s; 0 KCl, 0.55 ± 0.09 s; $n = 6$, $P < 0.01$; Li *et al.* 2003). This modulation at an intracellular site can be considered a 'foot in the back door' mechanism or evidence for intracellular pore closure.

Previous results from other laboratories on closely related channels also show interactions that suggest C-type inactivation is accompanied by a significant intracellular conformational change. For a variety of voltage-gated K$^+$ channels the development of C-type inactivation prevents

the binding of drugs that act within the pore of the channel from the intracellular side (Castle *et al.* 1994; Wang *et al.* 1997; Ficker *et al.* 1998). This is similar to the interpretation that an extracellular conformational changes accompanies C-type inactivation because of the sensitivity to extracellular TEA (Armstrong, 1971; Hoshi *et al.* 1990, 1991; Choi *et al.* 1991; Yellen *et al.* 1991).

Mutations near the extracellular mouth of the pore which alter C-type inactivation are considered to be evidence that C-type inactivation involves closure of the extracellular mouth of the pore. Similarly, mutations near the intracellular mouth of the pore on S6 also change the properties of C-type inactivation (Castle *et al.* 1994; Wang & Wang, 1997; Li *et al.* 2003). Thus, all of the criteria that were used to demonstrate the involvement of the extracellular mouth of the pore in C-type inactivation are also fulfilled for implicating the intracellular mouth of the channel.

This study suggests that major physical changes in pore structure associated with C-type inactivation occur on the intracellular side of the channel. While this finding is surprising given the well-established involvement of the extracellular side, it should be somewhat expected. For example, cysteine scanning of the extracellular mouth of the channel has only revealed residues that become more, not less, accessible during C-type inactivation (Liu *et al.* 1996). The linkage between N-type inactivation (which involves intracellular N-terminal binding) and C-type inactivation is also indicative of some coupling of events on the intracellular side to events on the extracellular side of the membrane (for a review see Rasmusson *et al.* 1998).

In order to account for a change in volume of the putative pore, movement of the transmembrane domain S6 is required (Doyle *et al.* 1998; Jiang *et al.* 2002). If S6 is a relatively rigid structure, such a model has the added benefit of explaining why mutations on the intracellular side of S6 alter C-type inactivation (Li *et al.* 2003). Movement of S6 with C-type inactivation is also compatible with the observation of increased residue accessibility on the extracellular face of the channel during C-type inactivation (Liu *et al.* 1996). Similarly, either rotational or translational involvement of S6 can explain why mutations on the far extracellular side of S6 alter C-type inactivation (Hoshi *et al.* 1990, 1991; Busch *et al.* 1991) despite their putative physical remoteness from the extracellular mouth of the pore in the crystal structure. Perhaps most importantly, these results explain why channel blockers are excluded from binding by C-type inactivation (Castle *et al.* 1994).

An important question that remains is 'How tightly closed is the intracellular pore mouth during C-type inactivation?'. The initial 'closed' crystal structure of KcsA was sufficiently ambiguous to spur debate as to whether or not it was an open or closed channel (Doyle *et al.* 1998).

Our experiments demonstrate that a large change in pore volume is associated with development of C-type inactivation. Some investigators (Starkus *et al.* 1997, 1998; Kiss *et al.* 1999) have reported that Na^+ ions, which have smaller hydrated radii than K^+ ions, can permeate the C-type inactivated channel in the absence of potassium. It is possible that the pore closure measured here is incomplete enough to pass sodium ions. Alternatively, this may be a reflection of the differences between ion channel types, or the specific ionic conditions, which can alter the conformation, gating and selectivity properties of channels (Hille, 2001).

The term C-type inactivation was originally derived from the C-terminal splice variants, which determined the properties of inactivation that remained in the absence of N-type inactivation (Hille, 2001). In some channels, there may also be P-type inactivation (De Biasi *et al.* 1993), which may involve changes in the selectivity filter near the external pore mouth (Varga *et al.* 2002). Conventional C-type inactivation may occur later and stabilize the S4 domain (Olcese *et al.* 1997; Loots & Isacoff, 1998, 2000). The data presented in this paper were obtained from Kv1.4 channels, which in the wild-type exhibit only N- and C-type inactivation. The construct we examined, Kv1.4ΔN, has the N-terminal deleted, so the 'ball and chain' mechanism of N-type inactivation no longer functions. The inactivation that remains fulfills the criteria for C-type inactivation and has been well characterized (Rasmusson *et al.* 1995). The existence of re-opening currents in Kv1.4ΔN suggests that there may be immobilization of a portion of S4, which is consistent with the observed behaviour of C-type inactivation in *Shaker* channels (Olcese *et al.* 1997; Loots & Isacoff, 1998, 2000). Our data show that applied osmotic pressure promotes a return to the closed state through an electrically silent pathway, without altering the recovery rate. This is consistent with the hyposthesis that immobilization of S4 by C-type inactivation occurs in regions remote from the intracellular side of the membrane (Loots & Isacoff, 2000). Indeed, mutation near the extracellular side of S5 in *Shaker* K^+ channels has been suggested to affect both the development of C-type inactivation and movement of S4 through alteration of the rotational movement of the S6 transmembrane spanning domain (Larsson & Elinder, 2000; Ortega-Saenz *et al.* 2000).

Slow, or C-type, inactivation is common to virtually all voltage-gated ion channels, including Na^+, K^+ and Ca^{2+} channels. The specific action of all antiarrhythmic drugs (except β-blockers) depends critically on the state of the channel. This is true for many other drugs which act on excitable cells in other tissues, such as smooth muscle and neurons. Virtually all clinically employed voltage-dependent cation channel blockers interact with the S6 residues lining the permeation pathway from the

intracellular side of the membrane (for a review see Rasmusson *et al.* 1998). This region is critical in understanding binding specificity and use dependence. Understanding the large conformational change at the intracellular face of the channel which occurs during C-type inactivation is crucial to understanding the complex behaviour of antiarrhythmic drugs and their use dependence.

APPENDIX

Equilibrium analysis

1. Volume changes associated with inactivation. The Kv1.4ΔN channel can be modelled well with four closed states (C), an open state (O) and an inactivated state (I) (Comer *et al.* 1994; Wang *et al.* 2003):

$$C \rightleftharpoons C \rightleftharpoons C \rightleftharpoons C \rightleftharpoons O \rightleftharpoons I. \tag{A1}$$
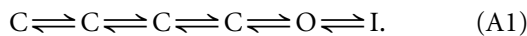
When a depolarization is applied to the channel the equilibrium will be well to the right in eqn (A1), so we considered only the dominant effect of osmotic pressure on inactivation. Following channel opening, C-type inactivation of Kv1.4ΔN channels is a single exponential process (Rasmusson *et al.* 1995) and can be simplified to a two-state process:

$$O \underset{}{\overset{K_\pi}{\rightleftharpoons}} I, \tag{A2}$$

where K_π is the osmotic pressure-sensitive equilibrium constant describing the reaction.

The ratio of the statistical probability of finding the channel in either the open or the inactivated state, $P_{open}/P_{inactivated}$, according to the Boltzmann distribution is related to the difference in free energy between the two states:

$$\frac{P_{open}}{P_{inactivated}} = \exp\left(\frac{G}{kT}\right), \tag{A3}$$

where G is the free energy difference between the two states under control conditions (Hille, 2001). When solutes too large to enter the mouth of the channel are introduced on one side of the membrane there will be a difference in osmotic pressure inside and outside the pore. This additional osmotic pressure leads to a change in the free energy difference between the two states, and the one with the smaller volume will be favoured. The extra energy term is equal to $\pi_{osm}\Delta V$, where π_{osm} is the difference in osmotic pressure inside and outside the channel, and ΔV is the change in solute-inaccessible volume between the open and closed states (Zimmerberg & Parsegian, 1986). The free energy change due to osmotic pressure is therefore:

$$\Delta G_\pi = \pi_{osm}\Delta V. \tag{A4}$$

When the channel is subjected to osmotic pressure, the probability of finding the channel in either the open or

inactivated state (cf. eqn (A3)) becomes:

$$\frac{P_{open,\pi}}{P_{inactivated,\pi}} = \exp\left(\frac{G}{kT}\right)\exp\left(\frac{\Delta G_\pi}{kT}\right), \tag{A5}$$

$$= \frac{P_{open}}{P_{inactivated}} \exp\left(\frac{\pi_{osm}\Delta V}{kT}\right). \tag{A6}$$

Rearranging:

$$\frac{P_{open,\pi}/P_{inactivated,\pi}}{P_{open}/P_{inactivated}} = \exp\left(\frac{\pi_{osm}\Delta V}{kT}\right). \tag{A7}$$

Taking the natural logarithm (ln) of both sides:

$$\ln\left(\frac{P_{open,\pi}/P_{inactivated,\pi}}{P_{open}/P_{inactivated}}\right) = \frac{\pi_{osm}\Delta V}{kT}. \tag{A8}$$

Rearranging:

$$\Delta V = \frac{kT}{\pi_{osm}}\ln\left(\frac{P_{open,\pi}/P_{inactivated,\pi}}{P_{open}/P_{inactivated}}\right). \tag{A9}$$

The ratio P_{open}/P_{closed} for a given depolarization can be estimated from the initial peak current, I_{peak}, and the steady-state current, I_{final} (extrapolated from the exponential fit of the inactivating experimental current to infinite time). This gives us the following equation (Hodgkin & Huxley, 1952):

$$P_{open}/P_{inactivated} = I_{final}/(I_{peak} - I_{final}). \tag{A10}$$

Substituting this in eqn (A9) gives:

$$\Delta V = \frac{kT}{\pi_{osm}} \ln\left(\frac{I_{final,\pi}/(I_{peak,\pi} - I_{final,\pi})}{I_{final}/(I_{peak} - I_{final})}\right). \tag{A11}$$

This allows us to estimate the change in solute-inaccessible aqueous volume associated with a change in osmotic pressure.

2. Volume changes associated with channel activation. Channel activation consists of multiple voltage-sensitive steps, and, generally, a final cooperative voltage-insensitive step (Hoshi *et al.* 1994). This complicates the analysis as applied to the simplified system described for inactivation described above. However, if we make the simplifying assumption that all of the volume change occurs at the final rate-limiting step of activation, the state model is simple:

$$C \rightleftharpoons O, \tag{A12}$$
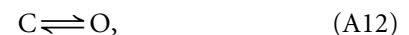
and the equation for calculating volume becomes similar to eqn (A9).

$$\Delta V = -\frac{kT}{\pi_{osm}} \ln\left(\frac{P_{open,\pi}/P_{closed,\pi}}{P_{open}/P_{closed}}\right). \tag{A13}$$

Since probabilities must sum to one, we know that:

$$P_{closed} = 1 - P_{open}, \tag{A14}$$

This can be used to reformulate eqn (A13) to give:

$$\Delta V = -\left(\frac{kT}{\pi_{\text{osm}}}\right)\ln\left(\frac{P_{\text{open},\pi}/(1 - P_{\text{open},\pi})}{P_{\text{open}}/(1 - P_{\text{open}})}\right). \tag{A15}$$

$$= -\left(\frac{kT}{\pi_{\text{osm}}}\right)\ln\left(\frac{P_{\text{open},\pi}/P_{\text{open}}}{(1 - P_{\text{open},\pi})/(1 - P_{\text{open}})}\right). \tag{A16}$$

The reduction in the probability of the channel being open once exposed to osmotic pressure, $P_{\text{open},\pi}$, can be calculated from the accompanying reduction in peak current, which is a whole cell measure of this change in probability:

$$P_{\text{open},\pi} = P_{\text{open}}(I_{\text{peak},\pi}/I_{\text{peak}}), \tag{A17}$$

One problem with the relationship given in eqn (A17) is that P_{open} is unknown for macroscopic currents, unless determined from single channel measurements. To date, only data from multichannel patches has been obtained from Kv1.4 or Kv1.4ΔN channels. In addition to the considerable uncertainty in our estimate of open probability and the simplifying assumption of a single step model of volume change, the measurement is subject to error if the open state as described in the model is a 'bursting' state that is a mixture of conducting and non-conducting states with similar volumes. However, if measurements are made only when:

$$P_{\text{open},\pi} < P_{\text{open}} \ll 1, \tag{A18}$$

then:

$$(1 - P_{\text{open},\pi})/(1 - P_{\text{open}}) \cong 1, \tag{A19}$$

and so eqn (A16) simplifies to:

$$\Delta V = -\frac{kT}{\pi_{\text{osm}}}\ln\left(\frac{P_{\text{open},\pi}}{P_{\text{open}}}\right). \tag{A20}$$

Substituting eqn (A17) into eqn (A20) yields:

$$\Delta V = -\frac{kT}{\pi_{\text{osm}}}\ln\left(\frac{I_{\text{peak},\pi}}{I_{\text{peak}}}\right). \tag{A21}$$

If P_{open} is sufficiently small, this free energy analysis can be shown to be independent of assumptions in the activation model (Almers, 1978). Because this approach requires analysis of very small conductances, potential difficulties include miscalculations caused by undetected changes in leak current and difficulties in interpretation introduced by the model of activation, if P_{open} is not sufficiently small.

3. Kinetic estimates of volume changes. Estimates of volume based on equilibrium analysis of channel open probabilities predict that transition rates between states should also be dependent on applied osmotic pressure. Because such estimates are dependent on kinetic changes instead of equilibrium analysis, the interpretation of such data is highly model dependent. However, such estimates are important, because they provide an additional check

on the assumptions of the equilibrium analysis. In general, because other steps may be rate limiting, kinetic estimates of volume changes may be less than or equal to the estimates obtained from equilibrium analysis.

The simplest model of transitions between a conducting and a non-conducting state is:

$$C \underset{k_{\text{close}}}{\overset{k_{\text{open}}}{\rightleftharpoons}} O, \tag{A22}$$

where the transitions between the two states at a constant potential are governed by k_{open}, the rate constant for the closed-to-open transition, and k_{close}, which is the rate constant for the open-to-closed transition. The time constant associated for relaxation between these two states is given by:

$$\tau = 1/(k_{\text{open}} + k_{\text{close}}). \tag{A23}$$

In the case of deactivation, where there are few, if any, re-openings and additional strongly voltage-dependent closed transitions are rapidly absorbing, eqn (A23) becomes well approximated by:

$$\tau_{\text{close}} \cong 1/k_{\text{close}}, \tag{A24}$$

or

$$k_{\text{close}} \cong 1/\tau_{\text{close}}. \tag{A25}$$

According to rate theory, k_{close} can be described as having an exponential dependence on a high-energy transition state:

$$k_{\text{close}} = A\exp\left(\frac{G}{kT}\right), \tag{A26}$$

where A is a constant associated with specific reaction conditions. If we assume that the energy-limiting step in this reaction contains the free energy associated with dehydrating the open pore (Hummer *et al.* 2001), then for applied osmotic pressure we can use the approximation:

$$k_{\text{close},\pi} = A\exp\left(\frac{G}{kT}\right)\exp\left(\frac{\Delta G_\pi}{kT}\right), \tag{A27}$$

$$= k_{\text{close}}\exp\left(\frac{\pi_{\text{osm}}\Delta V}{kT}\right). \tag{A28}$$

Substituting eqn (A25) into eqn (A28) gives:

$$1/\tau_{\text{close},\pi} = 1/\tau_{\text{close}}\exp\left(\frac{\pi_{\text{osm}}\Delta V}{kT}\right). \tag{A29}$$

Rearranging:

$$\Delta V = \left(\frac{kT}{\pi_{\text{osm}}}\right)\ln\left(\frac{\tau_{\text{close}}}{\tau_{\text{close},\pi}}\right). \tag{A30}$$

Similar arguments can be made for changes in the activation and inactivation rates.

Obviously, since the rate-limiting step may not involve the entire volume change, and the reverse transition also contributes to the time constant, kinetic estimates of volume changes from this equation may be an underestimate.

REFERENCES

Almers W (1978). Gating currents and charge movements in excitable membranes. *Rev Physiol Biochem Pharmacol* **82**, 96–190.

Armstrong CM (1971). Interaction of tetraethylammonium ion derivatives with the potassium channels of giant axons. *J Gen Physiol* **58**, 413–437.

Balser JR, Nuss HB, Chiamvimonvat N, Perez-Garcia MT, Marban E & Tomaselli GF (1996). External pore residue mediates slow inactivation in mu 1 rat skeletal muscle sodium channels. *J Physiol* **494**, 431–442.

Baukrowitz T & Yellen G (1995). Modulation of K^+ current by frequency and external $[K^+]$: tale of two inactivation mechanisms. *Neuron* **15**, 951–960.

Baukrowitz T & Yellen G (1996*a*). Two functionally distinct subsites for the binding of internal blockers to the pore of voltage-activated K^+ channels. *Proc Natl Acad Sci U S A* **93**, 13357–13361.

Baukrowitz T & Yellen G (1996*b*). Use-dependent blockers and exit rate of the last ion from the multi-ion pore of a K^+ channel. *Science* **271**, 653–656.

Bezanilla F, Perozo E, Papazian DM & Stefani E (1991). Molecular basis of gating charge immobilization in Shaker potassium channels. *Science* **254**, 679–683.

Busch AE, Hurst RS, North RA, Adelman JP & Kavanaugh MP (1991). Current inactivation involves a histidine residue in the pore of the rat lymphocyte potassium channel RGK5. *Biochem Biophys Res Commun* **179**, 1384–1390.

Castle NA, Fadous SR, Logothetis DE & Wang GK (1994). 4-Aminopyridine binding and slow inactivation are mutually exclusive in rat Kv1.1 and Shaker potassium channels. *Mol Pharmacol* **46**, 1175–1181.

Choi KL, Aldrich RW & Yellen G (1991). Tetraethylammonium blockade distinguishes two inactivation mechanisms in voltage-activated K^+ channels. *Proc Nat Acad Sci U S A* **88**, 5092–5095.

Comer MB, Campbell DL, Rasmusson RL, Lamson DR, Morales MJ, Zhang Y & Strauss HC (1994). Cloning and characterization of an Ito-like potassium channel from ferret ventricle. *Am J Physiol* **267**, H1383–1395.

De Biasi M, Hartmann HA, Drewe JA, Taglialatela M, Brown AM & Kirsch GE (1993). Inactivation determined by a single site in K^+ pores. *Pflugers Arch* **422**, 354–363.

Demo SD & Yellen G (1991). The inactivation gate of the Shaker K^+ channel behaves like an open-channel blocker. *Neuron* **7**, 743–753.

Doyle DA, Morais CJ, Pfuetzner RA, Kuo A, Gulbis JM, Cohen SL, Chait BT & MacKinnon R (1998). The structure of the potassium channel: molecular basis of K^+ conduction and selectivity. *Science* **280**, 69–77.

Ficker E, Jarolimek W, Kiehn J, Baumann A & Brown AM (1998). Molecular determinants of dofetilide block of HERG K^+ channels. *Circ Res* **82**, 386–395.

Hilgemann DW (1990). Regulation and deregulation of cardiac Na^+-Ca^{2+} exchange in giant excised sarcolemmal membrane patches. *Nature* **344**, 242–245.

Hille B (2001). *Ion Channels of Excitable Membranes*, third edn. Sinauer Associates Inc, Sunderland, MA, USA.

Hodgkin AL & Huxley AF (1952). A quantitative description of membrane current and its application to conduction and excitation in nerve. *J Physiol* **117**, 500–544.

Hoshi T, Zagotta WN & Aldrich RW (1990). Biophysical and molecular mechanisms of Shaker potassium channel inactivation. *Science* **250**, 533–538.

Hoshi T, Zagotta WN & Aldrich RW (1991). Two types of inactivation in Shaker K^+ channels: effects of alterations in the carboxy-terminal region. *Neuron* **7**, 547–556.

Hoshi T, Zagotta WN & Aldrich RW (1994). Shaker potassium channel gating. I: Transitions near the open state. *J Gen Physiol* **103**, 249–278.

Hummer G, Rasaiah JC & Noworyta JP (2001). Water conduction through the hydrophobic channel of a carbon nanotube. *Nature* **414**, 188–190.

Jiang Y, Lee A, Chen J, Cadene M, Chait BT & MacKinnon R (2002). The open pore conformation of potassium channels. *Nature* **417**, 523–526.

Kiss L, Loturco J & Korn SJ (1999). Contribution of the selectivity filter to inactivation in potassium channels. *Biophys J* **76**, 253–263.

Larsson HP & Elinder F (2000). A conserved glutamate is important for slow inactivation in K^+ channels. *Neuron* **27**, 573–583.

Li XY, Bett GKL, Jiang XJ, Bondarenko VE, Morales MJ & Rasmusson RL (2003). Regulation of N- and C-type inactivation by pHo and potassium in normal and mutant Kv1.4 channels: evidence for transmembrane communication. *Am J Physiol Heart Circ Physiol* **284**, H71–80.

Lipkind GM, Hanck DA & Fozzard HA (1995). A structural motif for the voltage-gated potassium channel pore. *Proc Natl Acad Sci U S A* **92**, 9215–9219.

Liu Y, Jurman ME & Yellen G (1996). Dynamic rearrangement of the outer mouth of a K^+ channel during gating. *Neuron* **16**, 859–867.

Loots E & Isacoff EY (1998). Protein rearrangements underlying slow inactivation of the Shaker K^+ channel. *J Gen Physiol* **112**, 377–389.

Loots E & Isacoff EY (2000). Molecular coupling of S4 to a K(+) channel's slow inactivation gate. *J Gen Physiol* **116**, 623–636.

Lopez-Barneo J, Hoshi T, Heinemann SH & Aldrich RW (1993). Effects of external cations and mutations in the pore region on C-type inactivation of Shaker potassium channels. *Receptors Channels* **1**, 61–71.

Naranjo D & Miller C (1996). A strongly interacting pair of residues on the contact surface of charybdotoxin and a Shaker K^+ channel. *Neuron* **16**, 123–130.

Olcese R, Latorre R, Toro L, Bezanilla F & Stefani E (1997). Correlation between charge movement and ionic current during slow inactivation in Shaker K^+ channels. *J Gen Physiol* **110**, 579–589.

Ortega-Saenz P, Pardal R, Castellano A & Lopez-Barneo J (2000). Collapse of conductance is prevented by a glutamate residue conserved in voltage-dependent K(+) channels. *J Gen Physiol* **116**, 181–190.

Perozo E, Cortes DM & Cuello LG (1999). Structural rearrangements underlying K^+-channel activation gating. *Science* **285**, 73–78.

Qu Y, Rogers JC, Chen SF, McCormick KA, Scheuer T & Catterall WA (1999). Functional roles of the extracellular segments of the sodium channel alpha subunit in voltage-dependent gating and modulation by beta1 subunits. *J Biol Chem* **274**, 32647–32654.

Rasmusson RL, Morales MJ, Castellino RC, Zhang Y, Campbell DL & Strauss HC (1995). C-type inactivation controls recovery in a fast inactivating cardiac K^+ channel (Kv1.4) expressed in *Xenopus* oocytes. *J Physiol* **489**, 709–721.

Rasmusson RL, Morales MJ, Wang S, Liu S, Campbell DL, Brahmajothi MV & Strauss HC (1998). Inactivation of voltage-gated cardiac K^{+} channels. *Circ Res* **82**, 739–750.

Rayner MD, Starkus JG, Ruben PC & Alicata DA (1992). Voltage-sensitive and solvent-sensitive processes in ion channel gating. Kinetic effects of hyperosmolar media on activation and deactivation of sodium channels. *Biophys J* **61**, 96–108.

Ruppersberg JP, Frank R, Pongs O & Stocker M (1991). Cloned neuronal IK(A) channels reopen during recovery from inactivation. *Nature* **353**, 657–660.

Starkus JG, Kuschel L, Rayner MD & Heinemann SH (1997). Ion conduction through C-type inactivated Shaker channels. *J Gen Physiol* **110**, 539–550.

Starkus JG, Kuschel L, Rayner MD & Heinemann SH (1998). Macroscopic Na^{+} currents in the "Nonconducting" Shaker potassium channel mutant W434F. *J Gen Physiol* **112**, 85–93.

Starkus JG, Schlief T, Rayner MD & Heinemann SH (1995). Unilateral exposure of Shaker B potassium channels to hyperosmolar solutions. *Biophys J* **69**, 860–872.

Todt H, Dudley SC Jr, Kyle JW, French RJ & Fozzard HA (1999). Ultra-slow inactivation in mu1 Na^{+} channels is produced by a structural rearrangement of the outer vestibule. *Biophys J* **76**, 1335–1345.

Varga Z, Rayner MD & Starkus JG (2002). Cations affect the rate of gating charge recovery in wild-type and W434F Shaker channels through a variety of mechanisms. *J Gen Physiol* **119**, 467–485.

Wang S, Morales MJ, Liu S, Strauss HC & Rasmusson RL (1997). Modulation of HERG affinity for E-4031 by [K^{+}]o and C-type inactivation. *FEBS Lett* **417**, 43–47.

Wang S, Morales MJ, Qu Y, Bett GCL, Strauss HC & Rasmusson RL (2003). Kv1.4 channel block by quinidine: evidence for a drug-induced allosteric effect. *J Physiol* **546**, 387–401.

Wang SY & Wang GK (1997). A mutation in segment I-S6 alters slow inactivation of sodium channels. *Biophys J* **72**, 1633–1640.

Yellen G, Jurman ME, Abramson T & MacKinnon R (1991). Mutations affecting internal TEA blockade identify the probable pore-forming region of a K^{+} channel. *Science* **251**, 939–942.

Zeuthen T, Zeuthen E & Klaerke DA (2002). Mobility of ions, sugar, and water in the cytoplasm of *Xenopus* oocytes expressing Na^{+}-coupled sugar transporters (SGLT1). *J Physiol* **542**, 71–87.

Zhang JF, Ellinor PT, Aldrich RW & Tsien RW (1994). Molecular determinants of voltage-dependent inactivation in calcium channels. *Nature* **372**, 97–100.

Zimmerberg J, Bezanilla F & Parsegian VA (1990). Solute inaccessible aqueous volume changes during opening of the potassium channel of the squid giant axon. *Biophys J* **57**, 1049–1064.

Zimmerberg J & Parsegian VA (1986). Polymer inaccessible volume changes during opening and closing of a voltage-dependent ionic channel. *Nature* **323**, 36–39.